COMMUNICATION

ChemComm
www.rsc.org/chemcomm

Electronic state and three-dimensional structure of Mn(III) active sites in manganese-containing aluminophosphate molecular sieve catalysts for the oxyfunctionalisation of alkanes†

Furio Corà,* Gopinathan Sankar,* C. Richard A. Catlow and John Meurig Thomas
Davy Faraday Research Laboratory, The Royal Institution of GB, 21 Albemarle Street, London, UK W1S 4BS. E-mail: sankar@ri.ac.uk

Received (in Cambridge, UK) 5th November 2001, Accepted 7th February 2002
First published as an Advance Article on the web 11th March 2002

Combined *in situ* X-ray absorption spectroscopy measurements and quantum mechanical calculations yield a quantitative three-dimensional structure of the tetrahedrally coordinated Mn(III) active sites in MnAlPO catalysts.

Although it is rare for Mn(III) ions to remain stably bound in four-coordination in oxides or other crystalline matrices, there is strong evidence that four-coordinated Mn(III) ions do exist in the framework sites of open-structured aluminophosphates (AlPOs).[1,2] Thus, in AlPO-18 and its polymorphic analogue AlPO-34, which are closely related to the zeolitic aluminosilicate chabazite, in AlPO-5 and in AlPO-36, manganese ions may occupy a small fraction of the Al(III) sites. Such ions constitute catalytically active sites for the regioselective oxidation of linear alkanes by air or oxygen at low temperatures.[3,4] In practice, it is convenient to introduce manganese into the AlPO framework sites as Mn(II) ions during the synthesis and to raise them to the Mn(III) state by subsequent calcination in oxygen. In some AlPOs, notably AlPO-18, all the Mn(II) ions initially introduced are converted to Mn(III) ions.[1,5] In this paper we first characterise the structural and electronic features of the Mn dopants with a combined experimental and computational study. This information is employed to quantify the number of catalytically active sites in different microporous Mn–AlPO catalysts.

To determine the local structure of Mn ions, we employed X-ray absorption spectroscopy (XAS), since this technique is element-specific and, unlike XRD, does not depend on the long-range order in the structure.[6] Despite providing average values over the whole catalyst, the bond distances and local environment derived from X-ray absorption near edge structure (XANES) and extended X-ray absorption fine structure (EXAFS) yield reliable descriptions of the electronic and geometric state of the dopant ions.[7] By relating this knowledge on the dopant ions to catalytic function, it is possible to pin down the structure of the active sites and characterise the reaction mechanism. However, in the absence of crystallographically well-characterised model systems that represent a typical coordination geometry of the dopant ions, it is difficult to associate the structure derived from XAS with an electronic state of the metal ions. This is indeed the situation with Mn-doped aluminophosphate catalysts, since very little is known about tetrahedrally coordinated Mn(III) ions. (There are few reports of EPR studies of MnAlPO catalysts,[8,9] but these are limited to large-pore materials where our previous studies with cobalt-doped systems suggest that only a small fraction of dopant ions is present in higher oxidation state.[10])

Mn K-edge XAS studies‡ of MnAlPO-18 show that, in the as-prepared catalyst containing 4 at% Mn, Mn(II) ions are present in tetrahedral coordination, with an average Mn–O distance of 2.02 ± 0.02 Å.[6,11] Upon heating this catalyst in oxygen, at *ca.* 550 °C, to remove the occluded organic template molecules, the white catalyst turns a violet-blue colour. *In situ* Mn K-edge XANES clearly shows the shift in edge position (see Fig. 1) to a higher energy; and, combined with the shorter Mn–O distance of 1.85 ± 0.02 Å derived from EXAFS (see Table 1), suggests that the oxidation state of the manganese is raised. Although it is reasonable to interpret these changes as the formation of Mn(III) ions in framework Al(III) sites, this is difficult to conclude unambiguously, since very little is known about tetrahedrally coordinated Mn(III). In addition, the different average Mn–O distances obtained for the calcined form of various microporous AlPO frameworks (see Table 2) further complicates the accurate determination of the structure of manganese ions in the active catalysts.

In order to understand the experimental findings and to determine the electronic state and three-dimensional structure

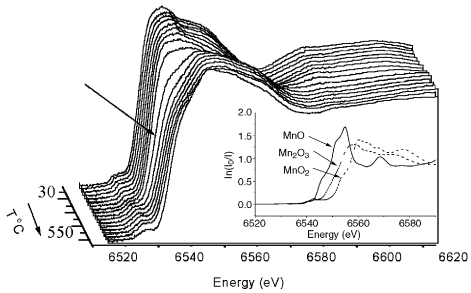

Fig. 1 Stacked Mn K-edge XANES recorded during the calcination process of MnAlPO-18 catalyst. The temperature range in which the absorption edge shifts to a higher energy is shown by an arrow. The inset shows the XANES data of the related oxide systems, MnO, Mn_2O_3 and MnO_2.

Table 1 Comparison of computed Mn(III)–O distances with the average distance derived from *in situ* EXAFS data

Ion type	Computed Mn–O bond distances[a]/Å				$<R>$/Å
Mn(III) high-spin	1.836	1.854	1.886	1.895	1.868
Mn(III) low-spin	1.843	1.846	1.848	1.852	1.847
EXAFS	—	—	—	—	1.85[b]

[a] The computational settings employed provide a reproduction to within 0.005 Å of the equilibrium bond-distances in perfect AlPO frameworks.[15] [b] The error involved in the EXAFS-determined bond distance is *ca.* ±0.02 Å. The coordination number is 4 and the Debye–Waller factor, σ^2 = 0.004 Å^2.

Table 2 Average Mn–O distance, R_{EXAFS} (Å), derived from our EXAFS data of calcined catalysts, fraction x of Mn ions present in the +3 state, and catalytic performance for different MnAlPO molecular sieve catalysts

	R_{EXAFS} (±0.02)	x (±0.12)	Catalytic conversion[a]
MnAlPO-18	1.85	1.00	16.08
MnAlPO-36	1.89	0.81	15.20
MnAlPO-5	1.92	0.63	13.75

[a] Conversion is given in mmole^{-1} (see ref. 12).

† Electronic supplementary information (ESI) available: Details of the experiment and data analysis. Table S1: structural parameters obtained for calcined MnAlPO-18 from EXAFS data analysis. Fig. S1: QM derived and experimental EXAFS data. Fig. S2: FT of the refined EXAFS data. See http://www.rsc.org/suppdata/cc/b1/b110017c/

DOI: 10.1039/b110017c

of the active Mn(III) ions, we carried out a detailed quantum mechanical (QM) study. The computational method adopted here describes the microporous AlPO framework *via* periodic boundary conditions, which provide a correct account of the extended nature of the catalyst. Although the experimental results are for MnAlPO-18, computational work has been performed on its close analogue AlPO-34, which has a smaller primitive unit-cell. (Both polymorphs are built up from chabazite cages, with the only difference being the way in which the double six ring units are oriented; the pore dimensions and cage structures are otherwise identical.) Previous work[12] on Co-doped materials has shown that EXAFS-derived distances in CoAlPO-18 and CoAlPO-34 were identical and that the two catalysts have similar regioselectivity and activity for n-hexane oxidation. It is therefore reasonable to expect the local Mn structure derived for MnAlPO-34 and MnAlPO-18 to be very similar. Calculations on substitutional Mn ions have been performed using a two-step procedure: first relaxing the AlPO matrix around the Mn(III) ion with interatomic potentials (IP) techniques;[13] this step includes the expansion of the unit cell parameters, needed to accommodate the steric strain introduced by the larger Mn dopants. The relaxed structure obtained from the IP study was then refined with periodic QM calculations, in which no constraint is imposed on the electronic configuration of Mn, except for its spin multiplicity. Both high- and low-spin Mn(III) sites were investigated. In view of the cost of the *ab-initio* QM calculations, only a partial relaxation of the structure around the Mn defect has been performed, which involves the Mn ion, its four nearest oxygens and the next-nearest phosphorus ions. Since the starting geometry obtained from the IP results already accounts for the long-range relaxation of the AlPO matrix around the Mn ions, such a constrained optimisation performed at the QM level is expected to yield a very accurate prediction of the local Mn environment. For the QM calculations, we chose the Hartree–Fock (HF) Hamiltonian, as implemented in the code CRYSTAL.[14] The basis set employed to describe the ions of the host AlPO framework is from elsewhere[15] and Mn dopants are described with a good quality, 86-411d41G basis set,[16] derived from previous studies of Mn oxides. The HF Hamiltonian includes the exact expression for exchange forces, and is expected to describe correctly the stable spin-state of the Mn ions.

The computed Mn(III)–O distances in AlPO-34 are given in Table 1 for both high- and low-spin electronic configurations. It is difficult to conclude from EXAFS alone whether we have low-spin or high-spin Mn(III) ions present in the structure, since the differences in the average Mn–O distance obtained from the computational method for these two states are within the uncertainty associated with the determination of bond distances (±0.02 Å) by EXAFS. We can, however, conclude that the high-spin Mn(III) ions predominate because our calculations predict this electronic state to be energetically stable (by *ca.* 3 eV) compared to low-spin Mn(III). Taking the structure obtained from the quantum chemical study as the starting point, we fitted the EXAFS data employing the multiple scattering procedure and the best fit obtained from this analysis is shown in Fig. 2(a). This procedure yields the final structure of the active catalyst shown in Fig. 2(b). The average Mn–O bond distance (shown in Table 1) can be effectively used to describe the environment and oxidation state of the catalytic centre.

The results of the QM calculations also permit rationalisation of the Mn–O distances in other MnAlPO alkane oxidation catalysts, such as MnAlPO-5 and MnAlPO-36. As in the interpretation of several CoAlPO catalysts,[10] we rationalise the different Mn–O distances obtained from EXAFS as being the weighted average between Mn(II)–O and Mn(III)–O distances. Using the average Mn–O values derived from the theoretical and experimental work, we estimate the fraction (x) of manganese ions that participate in the redox reaction, using the same relationship reported for CoAlPO catalysts:[10]

$$R_{\mathrm{EXAFS}} = xR_{\mathrm{Mn(III)}} + (1 - x)R_{\mathrm{Mn(II)}},$$

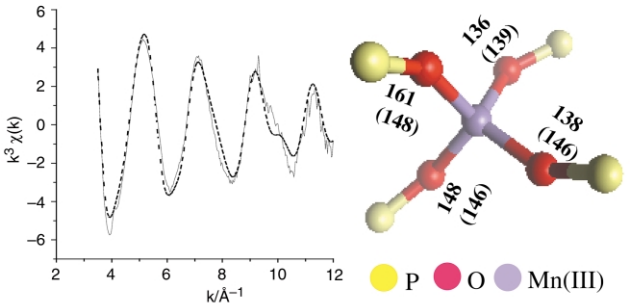

Fig. 2 (a) The best fit obtained, between the experimental (solid line) and the calculated (dashed line) EXAFS obtained by refining Mn–O, Mn–P distances, Debye–Waller factors and Mn–O–P bond angles, employing multiple scattering procedures. (b) The local structure of Mn(III) obtained from analysis of the EXAFS data. We have shown only the Mn–O–P bond angles derived from the calculations (in brackets) and from the EXAFS refinement. The Mn(III)–O distances are given in Table 1. QM derived and experimental EXAFS data are compared in ESI, in addition, the FT of the refined EXAFS data is also given in ESI.†

where $R_{\mathrm{Mn(II)}}$ is the Mn(II)–O and $R_{\mathrm{Mn(III)}}$ the Mn(III)–O distance, and R_{EXAFS} is the average Mn–O distance derived from EXAFS of the calcined catalyst. The Mn–O distance and the fraction x of Mn ions present as Mn(III) in the calcined catalysts are listed in Table 2, along with the conversion for dodecane oxyfunctionalisation.[12] In some systems, not all of the Mn(II) ions introduced in the catalyst during the synthesis are oxidised to Mn(III) in the activated catalyst, so that lesser amounts of Mn ions participate in the catalytic reaction. As with CoAlPO molecular sieve catalysts, good correlations exist between the fraction x and the catalytic conversion confirming that only those Mn ions that can be raised to a higher oxidation state by molecular oxygen are catalytically active.

We thank EPSRC for financial support and CLRC for facilities at Daresbury. G. S. thanks the Leverhulme Trust for a senior research fellowship, and F. C. thanks EPSRC for an advanced research fellowship.

Notes and references

‡ *In situ* combined XRD/XAS data were collected at station 9.3 of Daresbury SRS laboratory which operates at 2 GeV with a typical current in the range of 150–250 mA. Details of the experiment and data analysis are given as ESI.†

1 J. M. Thomas, R. Raja, G. Sankar and R. G. Bell, *Nature*, 1999, **398**, 227.
2 J. M. Thomas, R. Raja, G. Sankar and R. G. Bell, *Acc. Chem. Res.*, 2001, **34**, 191.
3 C. L. Hill, *Activation and Functionalisation of Alkanes*, Wiley, Chichester, 1989.
4 K. M. Waltz and J. F. Hartwig, *J. Am. Chem. Soc.*, 2000, **122**, 11 358.
5 G. Sankar and J. M. Thomas, *Top. Catal.*, 1999, **8**, 1.
6 G. Sankar, J. M. Thomas and C. R. A. Catlow, *Top. Catal.*, 2000, **10**, 255.
7 D. C. Koningsberger and R. Prins, *X-Ray Absorption: Principles, Applications, Techniques of EXAFS, SEXAFS and XANES*, Wiley, New York, 1986.
8 D. Y. Zhao, Z. H. Luan and L. Kevan, *J. Phys. Chem. B*, 1997, **101**, 6943.
9 U. Lohse, A. Bruckner, E. Schreier, R. Bertram, J. Janchen and R. Fricke, *Microporous Mater.*, 1996, **7**, 139.
10 P. A. Barrett, G. Sankar, C. R. A. Catlow and J. M. Thomas, *J. Phys. Chem.*, 1996, **100**, 8977.
11 A. Tuel, I. Arcon, N. N. Tusar, A. Meden and V. Kaucic, *Microporous Mater.*, 1996, **7**, 271.
12 R. Raja and J. M. Thomas, *Chem. Commun.*, 1998, 1841.
13 J. D. Gale and N. J. Henson, *J. Chem. Soc., Faraday Trans.*, 1994, **90**, 3175.
14 V. R. Saunders, R. Dovesi, C. Roetti, M. Causa, N. M. Harrison, R. Orlando and C. M. Zicovich-Wilson, *CRYSTAL 98 User's Manual*, University of Torino, Italy, 1998.
15 F. Cora and C. R. A. Catlow, *J. Phys. Chem. B*, 2001, **105**, 10 278.
16 In www.ch.unito.it/ifm/teorica/Basis_Sets/manganese.htm.